Bulletin of the Seismological Society of America. Vol. 63, No. 1, pp. 189–209. February 1973

A PROCEDURE FOR ELUCIDATING FINE STRUCTURE OF THE CRUST AND UPPER MANTLE FROM SEISMOLOGICAL DATA

By Tuneto Kurita

ABSTRACT

A formulation is presented to elucidate the layered structure down to a depth of over 200 km from long-period body-wave records of teleseismic deep-focus earthquakes. This formulation utilizes the ratios of vertical to horizontal motions of *P* and *SV* waves, and the ratio of *SH* motion to horizontal motion of *SV* waves. A strong advantage of the basic assumption of this method is that a postulation of horizontal parallel layering is limited to a few hundred kilometers. A two-step procedure is proposed and justified which makes a separate determination of the structure of crust and upper mantle. In each step, the truncated transfer ratio is used in which factors naturally incorporated in observed spectra, such as finiteness of the record, data window, instrumental response, source function, and later phases are all taken into account. Methods are developed to evaluate effects of the noise and the deviation of the direction of wave approach on the transfer ratio. This formulation makes it possible to elucidate the fine, regionalized structure of the crust and upper mantle such as transitional layering and details of the upper-mantle low-velocity zone.

A routine procedure for determining fine structure of the crust and upper mantle around recording stations is proposed. This cyclic procedure is a combined study of all available seismological methods such as body-wave transfer ratios, surface-wave dispersion, travel times, and synthetic seismograms, and a study of body-wave transfer ratios is in the heart of it. This approach leads to an unambiguous estimation of the layered structure in the upper part of the Earth.

Introduction

In addition to considerable complexities in crustal structure, recent seismological studies have revealed significant regional variations in upper-mantle structure. Various methods have been used for the investigation of the velocity structure in the crust and upper mantle, and sometimes different methods have inferred different structures. Because of the nonuniqueness problem, the use of only one method may lead to an erroneous conclusion concerning the structure. Strictly speaking, any combination of the methods may still lack uniqueness. However, we can expect a more reliable model from a combined use of methods which provide constraints on different parameters of the model. There should exist a fast and powerful procedure to determine the structure by a serial and/or parallel use of some methods. In this paper, with the aid of the actual data processing of Kurita (1972a, b; 1973a, b), we will outline this procedure. Among the methods employed, the transfer ratio method will be revaluated and refined into the most powerful means to determine the fine, regionalized structure. The other methods are mostly well established.

Up to the present, crustal structure has been studied mainly from seismic refraction surveys, and upper-mantle structure, from surface-wave dispersion. Both methods are principally based on the assumption that the crust and upper mantle are composed of a stack of horizontal parallel layers over a wide stretch along which the relevant waves

travel. Therefore, the resultant structure represents an average feature over this stretch. It has become apparent, however, that this basic assumption is violated by the actual structure in most of the regions.

Needless to say, these methods have revealed the global regional variations in the crustal and upper mantle structure. The results are valuable for our method, in that they provide additional constraints on the parameters and make it more feasible to construct models for the inverse problem. Recently some detailed studies of the upper mantle have been made by using the derivative of travel-time curves (for example, Johnson, 1967) and synthetic seismograms (for example, Helmberger and Wiggins, 1971). These methods also are not free from the violation of the basic assumption of horizontal parallel layering.

The proposed method limits this postulation only to horizontal distances of less than 100 km for the determination of the crustal structure, and about 350 km for the upper mantle down to about 200 to 240 km. Whether these distances are still long or not depends on the relative length of the structural inhomogeneity and the relevant wavelength. For long-period body waves, these distances may not nullify an application of the method for most of the geological provinces except for some unfavorable situations, and the inferred structure can be a much better approximation to the real Earth than models obtained from the other methods.

When we assume a layered structure for the crust and upper part of the mantle and an unstructured substratum for the underlying mantle under the station, comparisons of the observational transfer ratio, i.e., the amplitude ratio and phase difference among the vertical and horizontal motions of observed body waves, with theoretical ones of assumed models calculated with the Thomson-Haskell matrix method, supply a useful means for estimating the parameters of the layered structure, as was shown by Kurita (1969a) for *P* waves and by Kurita and Mikumo (1971) for *S* waves. As discussed in Berzon (1965), a simultaneous use of the amplitude and phase spectra brings about a noticeable improvement in accuracy of determination of the structure, compared with the case when only the amplitude spectrum is used.

From amplitude spectra of long-period *P* waves, Phinney (1964) first attempted to estimate the crustal structure under ALQ and BEC. Fernandez and Careage (1968) evaluated the crustal thickness under the region around Saint Louis and ARE, and Kurita (1969a, b, 1970) obtained the structure under three stations in Japan from amplitude and phase spectra. Bonjer, Fuchs, and Wohlenberg (1970) studied the crustal structure under the East African Rift System, and Hasegawa (1971) evaluated the structure under the Yellowknife region. Rogers and Kisslinger (1972) estimated the crustal thickness under ANT and NNA. Attempts to infer the crustal structure from short-period *P* waves, such as Ellis and Basham (1968), Hasegawa (1970) and Bakun (1971), were complicated, because the near-surface structure with which short-period waves are strongly concerned is too complex to be approximated by a stack of horizontal parallel layers. Kurita and Mikumo (1971) proposed the utilization of *S* waves, and succeeded in selecting models among the models which could not be discriminated from *P*-wave studies (Kurita, 1971; Mikumo and Kurita, 1971). Following the formulation made in the present paper, Kurita (1972a, b, c) has obtained the structure down to about 220 km in the central and western United States from *P* and *S* waves observed at several WWSSN stations. The theoretical aspect of the method was treated by Leblanc (1967) who proposed the utilization of the truncated transfer function for the determination of fine crustal structure from short-period data, and Ishii and Ellis (1970) who studied the effect of a dipping layer on the amplitude ratio. Their study shows that for long-period *P* waves, the general feature of the amplitude ratio does not vary substantially with a dip angle as large as 10°. Rogers and Kisslinger (1972) also studied this problem, tested

by a model experiment, and applied to observed data. These studies favor our method in support of its applicability to even such regions as the continental margin. Introducing complex velocities, Kurita and Mikumo (1971) estimated the effect of dissipation on the transfer ratio.

Such observational studies as mentioned above are important also from the next standpoint. Since the completion of the Worldwide Standardized Seismograph Stations Network, extensive studies have been made on the source process of earthquakes from spectra of long-period records observed at these stations. In spite of laborious work, however, these studies have not totally succeeded mainly because of a considerable signal distortion by unknown complicated structures of the crust and upper mantle under these stations. Eventually, for further detailed studies, the determination of the fine configuration of the structure is necessary.

Formulation for an Inference of the Layered Structure from Body-Wave Spectra

Recent seismological researches have elucidated several prominent discontinuities in the upper mantle, the depth interval of which is an order of 100 km, compared with, at most, tens of kilometers for the crustal layering, and possible transitional layering of some of the discontinuities in the crust and upper mantle. So long as we continue to use the conventional method to derive the layered structure from body-wave spectra, we cannot elucidate the fine configuration of the structure both in the crust and upper mantle. We will make it possible by re-evaluating the method. In this study, we are mostly concerned with long-period waves with periods longer than about 5 sec.

Separate Determination of the Structure of the Crust and Upper Mantle

Transfer functions and, accordingly, transfer ratios for models which involve layering of the crust and upper mantle show very ragged shapes. Characteristically, they show a superposition of closely spaced peaks, which are due to large time lags corresponding to wide intervals of discontinuities in the upper mantle, on widely spaced peaks, which are due to small time lags involved when waves are multiply reflected in the crustal layers. Theoretically, we can determine the structure of the crust and upper mantle at the same time. Practically, however, the effects from both parts seem more or less coupled in the transfer ratio, and, therefore, some kind of separate determination of the layering of the crust and upper mantle is highly desirable. It would make it possible to locate the transitional boundaries and estimate their sharpness, especially for regions underlain by thick low-velocity sedimentary layers, the existence of which sharpens peaks of the transfer ratio. As shown in Table 1, there is evidence for the existence of a high-velocity horizon with *P*-wave velocities of about 8.4 to 8.5 km/sec at a depth of about 90 to 110 km in North America. This horizon, however, is considerably below the Moho and its effect is small as seen in Kurita (1972b). Therefore, separating the layering at the Moho, we propose a two-step procedure which is schematically shown in Figure 1: (A) First, although rigorously incorrect, we assume the upper mantle just beneath the crust to be unstructured and determine the layering in the crust. (B) Second, assuming that the wave is not modified by the deeper part of the mantle where a smooth increase in velocity with depth occurs and conversions of waves are negligibly small, we determine the layering in the upper mantle. At the second step, however, because the signal usually tapers off as time goes on and is masked by later phases, we cannot take the time length long enough to include the whole portion of the record pertinent to all discontinuities in the upper mantle. The depth down to which the structure can be elucidated is controlled by the

TABLE 1

HIGH-VELOCITY LID ZONE (HLZ) FOUND IN THE UPPER MANTLE OF NORTH AMERICA*

Reference	Region and/or profile	$V_{B\text{-}LZ}$[a] (km/sec)	$V_{T\text{-}HLZ}$[b] (km/sec)	$\Delta V_{T\text{-}HLZ}$[c] (km/sec)	$D_{T\text{-}HLZ}$[d] (km)	$V_{B\text{-}HLZ}$[e] (km/sec)	$V_{T\text{-}LVZ}$[f] (km/sec)	$\Delta V_{T\text{-}LVZ}$[g] (km/sec)	$D_{T\text{-}LVZ}$[h] (km)	$D_{B\text{-}LVZ}$[i] (km)
Roller and Jackson (1966)	Denver line†	8.2	8.5	0.3	105					
Green and Hales (1968)	Little Rock and Wichita lines‡, Central U.S.	8.07	8.33	0.26	89	8.38	8.25	0.13	134	159
Lewis and Meyer (1968)	West line,†‡ Northern U.S.	8.20	8.47	0.27	126	4.7 (V_s)	3.9[j] (V_s)	0.8 ($-\Delta V_s$)	126	220
Mereu and Hunter (1969)	Churchill line,‡ Canadian Shield	8.05	8.43 ±0.03	0.38	84±3			0.004	95	
Julian (1970)	Eastern North America‡	8.1		0.2	60			≲0.2	80	110
				~0.3	~90				~160	~210
	Western North America‡	7.9		~0.3	~100					140
										~160
Hales, Helsley, and Nation (1970)	Gulf of Mexico	7.9	8.6	0.7	57				80	150
										~200
Stauder and Nuttli (1970)	Eastern U.S.§	8.17	8.37[k]	0.20	97±10					
Hill (1971)	Columbia Plateau,‖ Washington	8.0	8.4	0.4	100			~0.6	110	140

* Information on the underlying low-velocity zone (LVZ) is also shown. †Lake Superior Experiment (1963). ‡Project Early Rise (1966). §Southern Illinois Earthquake (Nov. 9, 1968). ‖Greenbush Lake Experiment (1969). [a]V_p at the bottom of the lid zone. [b]V_p at the top of the HLZ. [c]Increase of V_p at the top of the HLZ. [d]Depth to the top of the HLZ. [e]V_p at the bottom of the HLZ. [f]V_p at the top of the LVZ. [g]Decrease of V_p at the top of the LVZ. [h]Depth to the top of the LVZ. [i]Depth to the bottom of the LVZ. [j]V_s below the LVZ is 5.0 km/sec. [k]No indication of an abrupt increase of V_s.

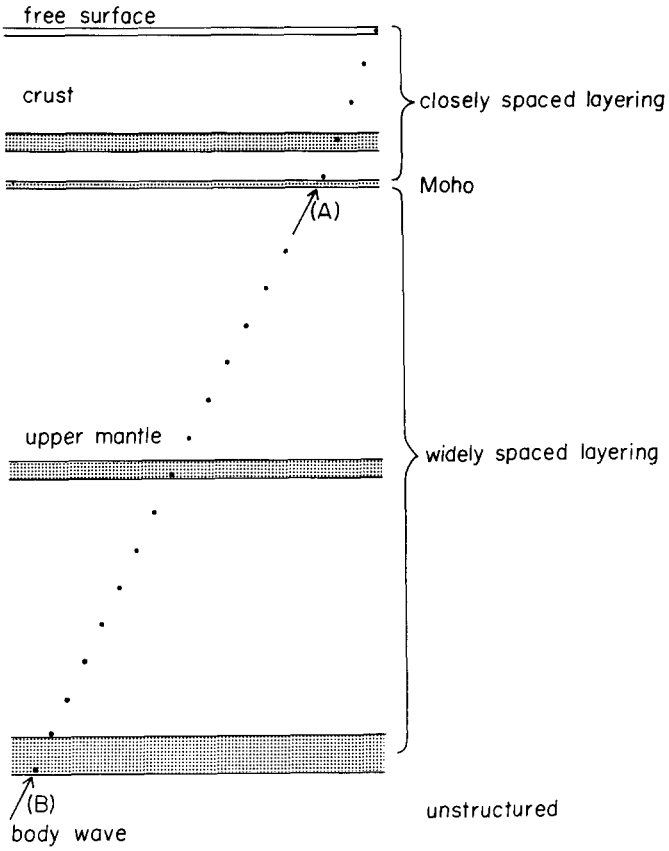

FIG. 1. Schematic representation of the layered structure of the crust and upper mantle assumed for the two-step procedure taken. Stippled stripes show the possible transitional layering.

time length which we can take. Because the discontinuities in the upper mantle are mostly widely spaced, we may be able to determine the layering to the depth corresponding to the adopted time length.

Each of the solid curves in Figure 2 shows the vertical and horizontal motions of the combined response of a crustal and upper-mantle model OXF71P and an instrument (15-100 Press-Ewing) on a plane P wave with $\delta(t)$ time function, incident from a teleseismic distance. As apparent from the insert, this model obtained in Kurita (1972b) for the structure southeast of OXF, Mississippi contains a well-developed low-velocity zone over the depth range from 119 to 196 km. The dashed curves show synthetic seismograms for model OXF71-SE-B. This model corresponds to the crustal part of model OXF71P, the crustal thickness of which is 43 km. The Fourier syntheses are made by using FFT for 256 (2^8) frequency bands of equal width of 0.0039 (2^{-8}) Hz between 0.0 and 1.0 Hz. The combined amplitude spectra are tapered off over higher frequencies by the superposition of the power spectral window

$$W(f) = 1 - |f|^{10} \quad |f| \leqq 1.0$$

and the time functions are calculated at intervals of 0.5 sec. In the figure undulations which appeared before the beginning of the time functions are arbitrarily removed. A comparison of these seismograms and the same kind of attempts for different models and different time functions justify our two-step procedure:

(A) The time function within a time length of about 40 sec includes most information on the layering in the crust, and is not much affected by discontinuities under the Moho. The horizontal time function usually suffers more contaminations from these discontinuities than the vertical time function.

(B) The time function within a time length of about 100 to 120 sec contains most of the effective reflections from the discontinuities down to about 200 to 240 km. This time function may not be significantly affected by the layering below the above depth or by discontinuities below the bottom of the low-velocity zone, because the next sharp discontinuity may be at least 100 km below its bottom, as apparent from Table 1 and other studies (for example, Johnson, 1967; Julian and Anderson, 1968; Johnson, 1969; Archambeau, Flinn, and Lambert, 1969; Whitcomb and Anderson, 1970; Helmberger and Wiggins, 1971). In this step, some adjustment on the crustal layering may be made.

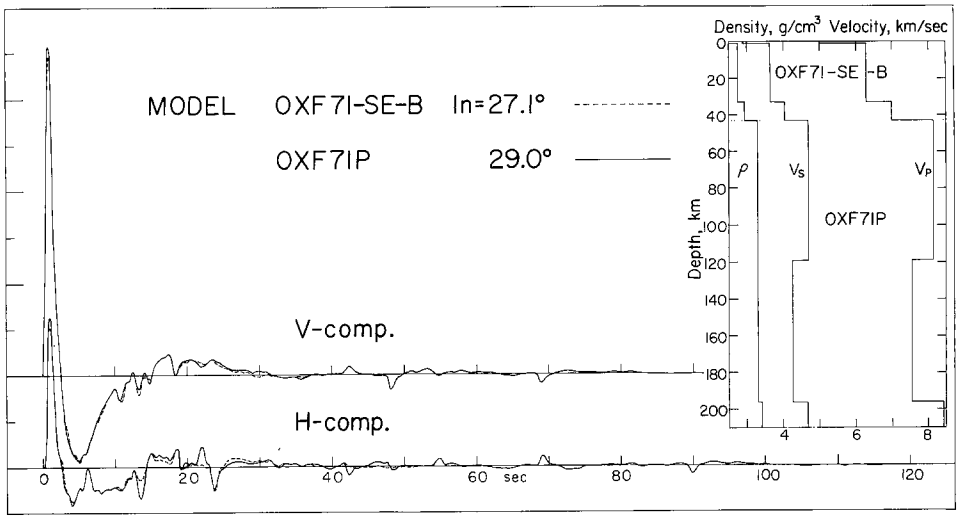

FIG. 2. Synthetic seismograms showing the vertical and horizontal motions of the combined response of the crustal and upper-mantle model, OXF71P and its crustal model, OXF71-SE-B, with a recording instrument (15–100 Press-Ewing) on a plane P wave with $\delta(t)$ time function for angles of incidence to the bottom of the models of 29.0° and 27.1°, respectively. These angles are taken to be consistent with Snell's law, and correspond to the epicentral distance of about 66° for the focal depth of 600 km. The models are shown in the insert and also schematically illustrated in Figure 1 except for the transitional layering.

There remains one problem about the resolution related to the comparatively short time length of analysis. If we use the power data window proposed by Kurita (1969c), which mostly passes the latter part of the signal, and take the time length of over about 100 sec, the observational transfer ratio does not show a substantial change with increased time length compared with a marked change for the time length shorter than about 100 sec, as is shown in Figure 2 of Kurita (1972b). This means that we can attain sufficient resolution in the above situation. Therefore, we take an effective time length of about 40 sec at the first step and about 100 to 120 sec at the second step, although rigorously the time length should differ for different underlying structure. Within the effective time length, the amplitude of the windowed signal is to be just above one half of the amplitude of the signal itself. In order to elucidate the structure down to a given depth, the time length required for S waves is at least one and a quarter times longer than that for P waves.

Utilization of Truncated Transfer Function

The observed spectrum of the direct body wave, $F(\omega)$ can be expressed as

$$F(\omega) = [S(\omega)\ M(\omega)\ U(\omega)\ L(\omega)\ I(\omega)] * W_T(\omega) \tag{1}$$

where $S(\omega)$ represents the source spectrum and is generally a function of spatial coordinates as well as the circular frequency, ω. $M(\omega)$, $U(\omega)$, and $L(\omega)$ are the response spectra of the layered structure around the source, the unstructured part of the mantle, and the layered structure under the station, respectively, and $I(\omega)$ is the instrumental response. $W_T(\omega)$ is the spectral window corresponding to a data window superposed on the record with a time length of T sec.

$U(\omega)$ may virtually represent the product of the divergence coefficient caused by geometrical spreading along the wave path, g, and the dissipation, $D(\omega)$,

$$U(\omega) = gD(\omega). \tag{2}$$

The expression for g is conventional. An excellent means for evaluating this coefficient and some results appear in Shimshoni and Ben-Menahem (1970). The expression for $D(\omega)$ is

$$D(\omega) = \exp\left[-\frac{\omega}{2}\int \frac{dp}{V(r)\ Q(r, \omega)}\right] \tag{3}$$

where $V(r)$ is the velocity as a function of the Earth's radius, and $Q(r, \omega)$ represents a relation of the Q value to depth and frequency. The integration is taken along the wave path.

We are concerned, here, with records of deep-focus earthquakes. This may make it possible to separate $S(\omega)$ into the spatial and temporal parts for long-period waves (Teng and Ben-Menahem, 1965; Archambeau, 1968), and to regard the effect of $M(\omega)$ as small. The former implies that the same time function is emitted from the source regardless of direction. When we make the conventional assumption that the Q value is independent of frequency, a tentative estimate based on the probable velocity and Q distributions for P waves shows that $D(\omega)$ decreases exponentially from 1 at 0.0 Hz to at least 0.5 at 0.2 Hz. If the Q value is linearly dependent on frequency as experimentally obtained by Kurita (1968), $D(\omega)$ is substituted for a constant. $S(\omega)$ should be estimated from empirical study. As will be apparent from an experimental study by Kurita (1973a), however, an evaluation of the combined spectrum of $S(\omega)$, $M(\omega)$, and $D(\omega)$ is simply made, but their separation is rather difficult. As far as the study of the structure under the recording station is concerned, this separation is unnecessary. Therefore, we represent this combined spectrum as $B(\omega)$,

$$B(\omega) = S(\omega)\ M(\omega)\ D(\omega) \tag{4}$$

which may correspond to the spectrum of the direct P or S phase incident at the base of the layered structure under the station. Accordingly, the ratio of the vertical to horizontal motions of the observed spectrum is represented as

$$\frac{F_w(\omega)}{F_u(\omega)} = \frac{[B(\omega)\ L_w(\omega)\ I_w(\omega)] * W_T(\omega)}{[B(\omega)\ L_u(\omega)\ I_u(\omega)] * W_T(\omega)} \tag{5}$$

where the subscripts, w and u, refer to the vertical and horizontal motions, respectively. Following the terminology of Leblanc (1967) who referred to the numerator and denominator of expression (6), below, as the truncated transfer function, we refer to expression (5) as the truncated transfer ratio.

Whereas the observed transfer ratio is obtained by expression (5), the theoretical transfer ratio is usually calculated by $L_w(\omega)/L_u(\omega)$ for the assumed layered model. Thereafter, both functions are compared. The discrepancy resulting from adoption of the different functions can be reduced by taking a long time length and utilizing an adequate data window. Leblanc (1967) showed that under two assumptions, expression (5) reduces to

$$\frac{F_w(\omega)}{F_u(\omega)} = \frac{L_w(\omega) * W_T(\omega)}{L_u(\omega) * W_T(\omega)} \tag{6}$$

and that the difference between this ratio and $L_w(\omega)/L_u(\omega)$ is negligible for the record with a long duration. Glover and Alexander (1969) proposed that the truncation effect may not be ignored for the study of the structure from long-period P waves, which is verified by actual analyses in Kurita (1972a, b). Because we cannot usually take the time length long enough, we should calculate the transfer ratio by using expression (5) or its expansion,

$$\frac{F_w(\omega)}{F_u(\omega)} = \frac{[B(\omega)\, L_w(\omega)\, I_z(\omega)] * W_T(\omega)}{[B(\omega)\, L_u(\omega)\, I_N(\omega)] * W_T(\omega) \cos\phi + [B(\omega)\, L_u(\omega)\, I_E(\omega)] * W_T(\omega) \sin\phi} \tag{7}$$

where ϕ is the azimuthal angle from the station to the event, and $I_z(\omega)$, $I_N(\omega)$, and $I_E(\omega)$, the instrumental response of Z, NS, and EW components of seismographs. This response can be evaluated from the response curve by the method described in Espinosa, Sutton, and Miller (1965). If the NS or EW record is absent or of poor quality, $[B(\omega)\, L_u(\omega)\, I_E(\omega)] * W_T(\omega)/\sin\phi$ or $[B(\omega)\, L_u(\omega)\, I_N(\omega)] * W_T(\omega)/\cos\phi$ can be substituted for the denominator, respectively.

The truncated transfer function can be calculated in two ways. The conventional method is simply to convolve the transfer function with the spectral window. When the data window such as Fejér kernel window, which heavily suppresses the latter part of the record, is superposed on the record, this method is much more convenient than the method described below, because the corresponding spectral window has no significant sidelobes, and the transfer function can be easily obtained by an averaging in the frequency domain. The main disadvantage is that this function cannot be estimated over the lowest-frequency range. However, for the data window which passes the latter part of the record, the corresponding spectral window has rather large effective sidelobes. Another method is composed of two successive Fourier transforms, as described in Leblanc (1967). For expression (6) the procedure is represented as

$$l_{u,w}(t) = \frac{1}{2\pi} \int_{-\infty}^{\infty} L_{u,w}(\omega) \exp(i\omega t)\, d\omega$$

$$\frac{F_w(\omega)}{F_u(\omega)} = \frac{\int_{-T}^{T} l_w(t)\, w_T(t) \exp(-i\omega t)\, dt}{\int_{-T}^{T} l_u(t)\, w_T(t) \exp(-i\omega t)\, dt}$$

where $w_T(t)$ is the data window, the Fourier pair of $W_T(\omega)$.

The truncated transfer ratio of SH motion to the horizontal motion of SV waves is expressed as

$$\frac{F_{SH}(\omega)}{F_u(\omega)} = \frac{[B(\omega)\, L_{SH}(\omega)\, I_N(\omega)] * W_T(\omega) \sin\phi - [B(\omega)\, L_{SH}(\omega)\, I_E(\omega)] * W_T(\omega) \cos\phi}{[B(\omega)\, L_u(\omega)\, I_N(\omega)] * W_T(\omega) \cos\phi + [B(\omega)\, L_u(\omega)\, I_E(\omega)] * W_T(\omega) \sin\phi} \tag{8}$$

where the denominator and numerator are the frequency domain correspondents of expressions (14) and (15), respectively.

Determination of the Time Length of Analysis in Relation to the Incidence of Later Phases

P phase. The above formulation is useful in each step only when we can get records of the *P* phase exclusive of all other phases, with a time length of about 40 and over 100 sec, respectively. However, this situation is generally not realized, as apparent from Figure 3. Therefore, we need to extend the time length by incorporating later phases.

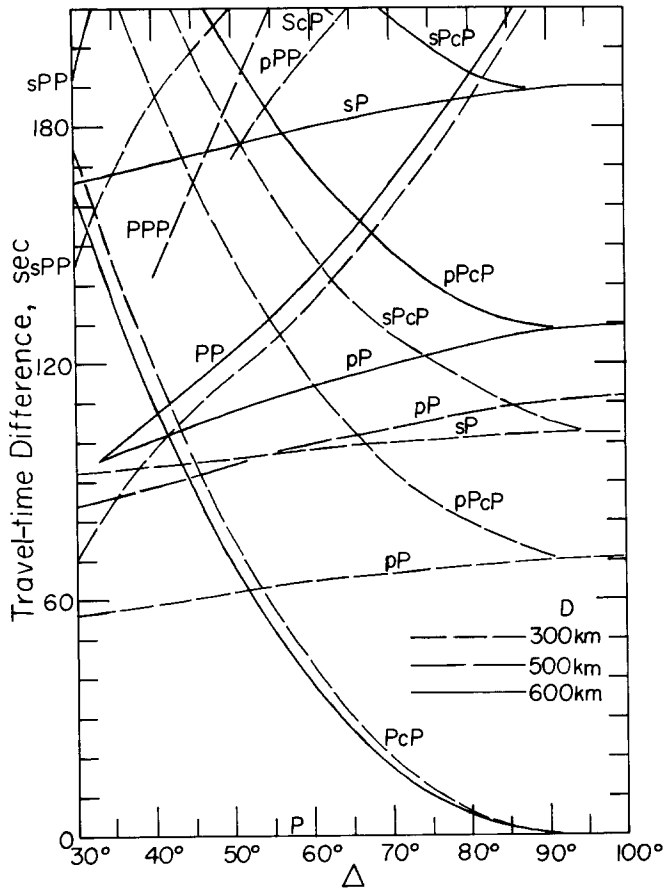

FIG. 3. Travel-time differences between the teleseismic direct *P* phase and major later phases for focal depths of 300, 500 (only for *pP*), and 600 km.

Figure 3 shows travel-time differences between the teleseismic direct *P* phase and major phases arriving within 3.5 min after the direct *P* phase for deep focal depths. Time differences for the *PcP*, *pP*, and *PP* phases are obtained from tables for *P* phases of Herrin *et al.* (1968), whereas those for the *sP* and *PPP* phases are calculated from tables of Jeffreys and Shimshoni (1964), and Jeffreys and Bullen (1940), respectively. *pPP*, *sPP*, *pPcP*, *sPcP* and *ScP* are based on travel-time curves of Gutenberg and Richter (1936). Some inconsistencies among the curves in the figure are inevitable due to the difference in the source of data.

Whereas phases reflected at the Earth's surface may be strongly distorted by the structure under the point of reflection, those reflected at the mantle-core boundary may not be distorted as much because of its sharp interface (Bolt, 1972; Phinney, 1972). Therefore, the *PcP* phase may be incorporated within the time length of analysis of the *P* phase, but phases such as *pP*, *sP*, and *PP* should not be included. Conversely, a possibility was suggested by Wu and Hannon (1966) that the layered structure under the point of reflection can be elucidated from the spectral analysis of *P* and *PP* phases after the correction of the response of the layered structure under the station.

As discussed above, an elucidation of the structure down to about 220 km is possible only from records with an available time length of about 100 sec or more. For the records of deep-focus earthquakes with depths of about 300 km, the *pP* phase has a strong onset at about 60 to 70 sec after the onset of the direct *P* phase. For those with depths of over about 500 km, however, we can take the time length of about 100 to 120 sec if we take into account the *PcP* phase. The effect of this phase on the transfer ratio of the *P* phase can be evaluated in two ways. Comparisons of the transfer ratios for different earthquakes and different time lengths, and the location of trough positions resulting from the *PcP* phase by the method described in Kurita (1969c), make it possible to estimate this effect. Because the signal amplitude of the *PcP* phase tapers off into that of the *P* phase with increased distance, and accordingly, troughs become less pronounced and appear widely spaced in the frequency domain, this effect can be better eliminated on records from more distant shocks. An alternative rigorous method is to incorporate the transfer ratio of the *PcP* phase into that of the *P* phase. The record section which is composed of the direct *P* phase, $f_p(t)$ and the *PcP* phase, $f_{PcP}(t)$, and superposed by the data window, $w_T(t)$ with a time length of T sec, is expressed as

$$f(t) = [f_P(t)+f_{PcP}(t-t_{PcP-P})]w_T(t) \tag{9}$$

where t_{PcP-P} is the difference in arrival time between the *P* and *PcP* phases. The fiducial time of $w_T(t)$ is taken at the arrival time of the *P* phase. The corresponding expression in the frequency domain is

$$F(\omega) = [F_P(\omega)+F_{PcP}(\omega)\exp(-i\omega t_{PcP-P})] * W_T(\omega) \tag{10}$$

where

$$F_P(\omega) = g_P\, B_P(\omega)\, L_P(\omega)\, I(\omega)$$

$$F_{PcP}(\omega) = g_{PcP}\, B_{PcP}(\omega)\, L_{PcP}(\omega)\, I(\omega)\, C(\omega)$$

$$B_{P,\,PcP}(\omega) = [S(\omega)\, M(\omega)\, D(\omega)]_{P,\,PcP}$$

and

$$D_{P,\,PcP}(\omega) = \exp\left[-\frac{\omega}{2}\int_{P,\,PcP}\frac{d_p}{V(r)\,Q(r,\omega)}\right].$$

$C(\omega)$ represents the complex reflection coefficient at the mantle-core boundary, which can be evaluated by the matrix formulation developed by Kanamori (1967) and Teng (1967). The relevant truncated transfer ratio is expressed as

$$\frac{F_w(\omega)}{F_u(\omega)} =$$

$$\frac{[B(\omega)\, L_w(\omega)\, I_w(\omega)]_P * W_T(\omega)+b\{[B(\omega)\, L_w(\omega)\, I_w(\omega)]_{PcP}\, C(\omega)\exp(-i\omega t_{PcP-P})\} * W_T(\omega)}{[B(\omega)\, L_u(\omega)\, I_u(\omega)]_P * W_T(\omega)+b\{[B(\omega)\, L_u(\omega)\, I_u(\omega)]_{PcP}\, C(\omega)\exp(-i\omega t_{PcP-P})\} * W_T(\omega)} \tag{11}$$

where $b = g_{PcP}/g_P$. For waves incident from the teleseismic distance, each term of $B_{PcP}(\omega)$ may be regarded as approximately the same as each $B_P(\omega)$. Therefore, we assume that

$$B_{PcP}(\omega) = B_P(\omega). \tag{12}$$

In this circumstance, the only difference in the first and second brackets of expression (11) is the angle of incidence of the relevant wave at the base of the layered structure under the station, i_n used in calculating $L(\omega)$. This angle depends more or less on the assumed model. However, the transfer ratio is not sensitive to the variation in angle of incidence, and we may adopt one of the proposed earth models.

Kanamori (1967) observed a marked resemblance of teleseismic short-period P phases to PcP phases, interpreted it as a small effect of the mantle-core boundary, and suggested the existence of a sharp interface, whereas Buchbinder (1968) showed that teleseismic long-period P and PcP phases have almost the same amplitude spectra. Recently Bolt (1972) and Phinney (1972) observed sharp reflections of short-period core phases, and estimated the thickness of the mantle-core boundary at less than a few kilometers. Accordingly, we may reasonably assume it as a first order discontinuity. Regarding this discontinuity as a plane solid-liquid interface, and following a similar procedure as described in Ewing, Jardetzky, and Press (1957), we obtain the reflection coefficient for an incident plane P wave in the mantle,

$$C = \frac{\rho_c/\rho_m - r_{\alpha c}/r_{\alpha m}[(1-\gamma_m)^2 - r_{\alpha m}\, r_{\beta m}\, \gamma_m{}^2]}{\rho_c/\rho_m + r_{\alpha c}/r_{\alpha m}[(1-\gamma_m)^2 + r_{\alpha m}\, r_{\beta m}\, \gamma_m{}^2]}$$

where

$$\begin{aligned} r_{\alpha m, \alpha c} &= [(c/\alpha_{m,\,c})^2 - 1]^{1/2} \\ r_{\beta m} &= [(c/\beta_m)^2 - 1]^{1/2} \\ \gamma_m &= 2(\beta_m/c)^2 \end{aligned}$$

and c is the horizontal phase velocity. Subscripts, m and c, are concerned with mantle and core, respectively. $r_{\alpha c}$ is a negative imaginary when $c < \alpha_c$. However, this situation is never realized at the mantle-core interface for the P wave incident from the mantle. Therefore, C is always real, and, only when C is negative, the phase shift occurs, the amount of which is always π. Figure 4 shows the reflection coefficient, $|C|$, and the phase shift, P, for three mantle-core interface models shown in Table 2. Because these estimates are obtained for the plane wave incident at the plane interface, they cannot closely approximate the real values for the angle of incidence at the interface, i_c, of over about 70° (Sato, 1969). However, the above formula is sufficient for the present purpose. Figure 5 shows i_c together with angle of incidence at the focus, i_d, of the P and PcP phases, for deep focal depths. i_d was calculated by Ritsema (1958) from the Jeffreys' velocity model, while i_c is calculated from i_d by means of Snell's law, the constancy of $r \sin i/\alpha$ along the wave path where r represents the distance from the Earth's center to the relevant depth. From Figures 4 and 5, it appears that the PcP phase arriving at the teleseismic distance up to about 90° does not suffer a phase shift at the mantle-core interface. Substituting C for $C(\omega)$ in expression (11), we have

$$\frac{F_w(\omega)}{F_u(\omega)} =$$

$$\frac{[B(\omega)\, L_w(\omega)\, I_w(\omega)]_P * W_T(\omega) + a\{[B(\omega)\, L_w(\omega)\, I_w(\omega)]_{PcP} \exp(-i\omega t_{PcP-P})\} * W_T(\omega)}{[B(\omega)\, L_u(\omega)\, I_u(\omega)]_P * W_T(\omega) + a\{[B(\omega)\, L_u(\omega)\, I_u(\omega)]_{PcP} \exp(-i\omega t_{PcP-P})\} * W_T(\omega)} \tag{13}$$

where $a = bC = g_{PcP}C/g_P$.

TABLE 2

MANTLE-CORE INTERFACE MODELS

Model	Parameter	Mantle	Core
Jeffreys	α (km/sec)	13.64	8.10
	β (km/sec)	7.30	0.00
	ρ (g/cm^3)	5.66	9.70
462159M	α (km/sec)	13.60	8.00
	β (km/sec)	7.00	0.00
	ρ (g/cm^3)	6.00	9.85
M0	β (km/sec)	7.25	0.00
	ρ (g/cm^3)	5.50	9.85

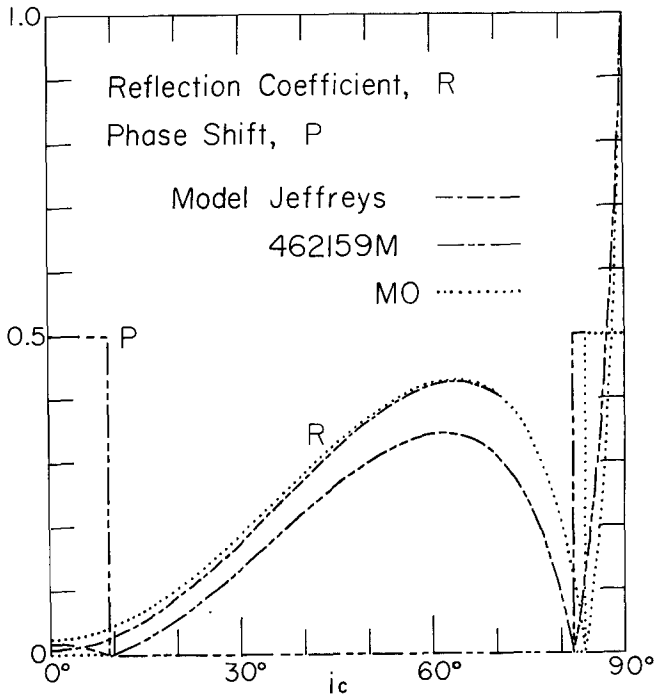

FIG. 4. Reflection coefficient and phase shift (in parts of circle) for a plane P wave incident at the assumed plane mantle-core interface models shown in Table 2.

However, Bolt (1972) and Phinney (1972) postulate a negative velocity zone above the sharp mantle-core interface over about 150 km and 30 km or less, respectively. Anderson and Jordan (1972), and Jordan and Anderson (1972) find a pronounced low-velocity, high-density zone at the base of the mantle mainly from differential travel-time and free oscillation studies.

This transition zone may have some effects on the incident P wave. The following discussion is based mainly on modified versions of model 462159, one of the mantle-core boundary models proposed by Anderson and Jordan (1972). It contains a linear transition zone extending over about 110 km. In this zone the S-wave velocity decreases from about

7.20 to 7.00 km/sec, and the density increases from about 5.45 to 6.00 g/cm^3, whereas the P-wave velocity is kept at about 13.60 km/sec. Among a suite of four models shown in Figure 6, model 462159M100 has almost the same configuration as model 462159 except for the thickness of the transition zone of 100 km. It is shown as the numerical suffix of model name. Figure 7 shows the reflection coefficient, $R(\omega)$, and the difference in the phase arrival time, $P(\omega)/\omega$, of any frequency from that at the low-frequency limit, $\lim_{\omega \to 0} P(\omega)/\omega$, for the P-wave incident at the top of mantle-core boundary models shown in Figure 6 and Table 2, with an angle of 60°. This angle corresponds to the epicentral

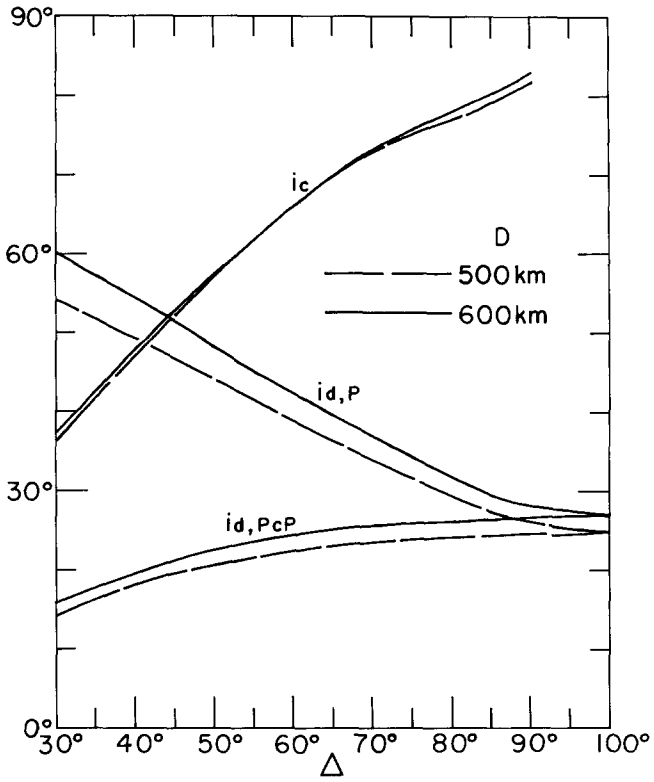

FIG. 5. Angle of incidence at the mantle-core interface, i_c for the P wave from deep-focus earthquakes. Angles of incidence at the focus, i_d for the P and PcP phases are shown for reference.

distance of about 53° for the focal depth of 500 to 600 km, as apparent from Figure 5. The absolute value of the last function, t_0 is zero for models 462159M and M0. For models 462159M20, M50, and M100, t_0 is 1.558, 3.896 (2.5 × 1.558), and 7.792 (5 × 1.558) sec, respectively, being proportional to the thickness of the transition zone. Defining

$$\begin{aligned} T(\omega) &= P(\omega)/\omega - \lim_{\omega \to 0} P(\omega)/\omega \\ &= P(\omega)/\omega + t_0 \end{aligned}$$

we have

$$\begin{aligned} C(\omega) &= R(\omega) \exp [iP(\omega)] \\ &= R(\omega) \exp [i\omega\, T(\omega)] \exp (-i\omega t_0). \end{aligned}$$

Although a simple substitution of this expansion for $C(\omega)$ in expression (11) produces $R(\omega) \exp [i\omega\, T(\omega)] \exp [-i\omega(t_{PcP-P} + t_0)]$, t_0 is intrinsically included in t_{PcP-P}. Therefore,

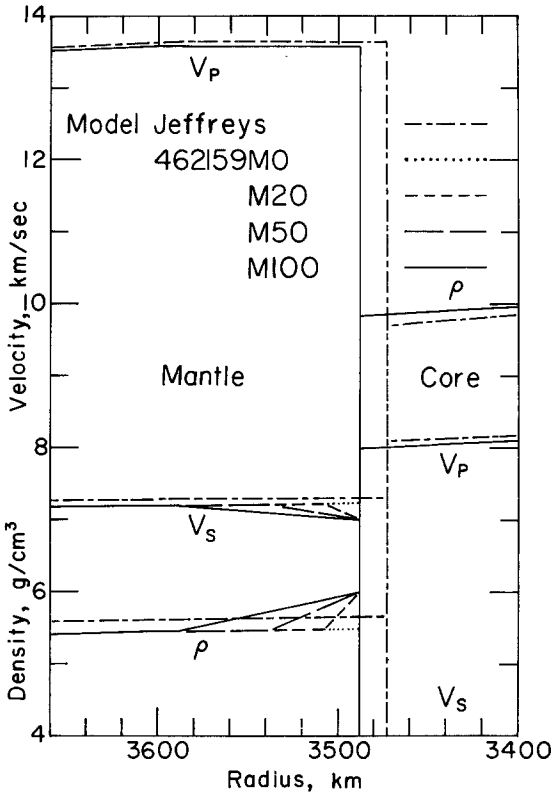

FIG. 6. Mantle-core boundary models. A suite of four models is a modified version of model 462159 proposed by Jordan and Anderson (1972).

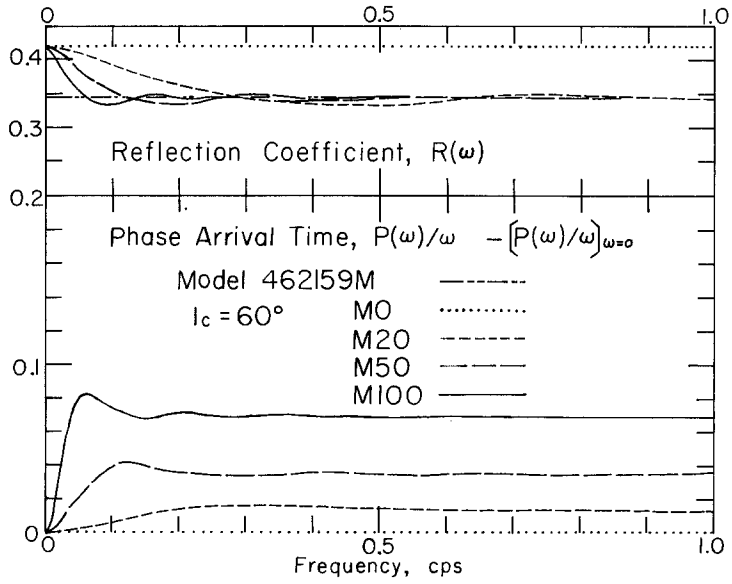

FIG. 7. Reflection coefficient and difference in phase arrival time of any period from that at the long-period limit in $1/2\pi$ sec, for the P wave incident at the top of mantle-core boundary models in Figure 6 and Table 2, with unit amplitude and an angle of 60°.

the effect of the transition zone on the incident P wave is mostly ascribed to $R(\omega)$ exp $[i\omega T(\omega)]$. $T(\omega)$ is concerned with frequency-dependency of travel time resulting from the increased phase shift caused by continuous diffraction through the transition zone (Kane, 1965). In the calculation of $R(\omega)$ and $T(\omega)$, the linearly transitional layer is treated as a limiting case $H/n \to 0$ of a step-wise structure of H km composed of n layers of equal thickness. In Figure 7, n is taken as 100, corresponding to the thickness of sublayer of 0.2, 0.5, and 1.0 km for models 462159M20, M50, and M100, respectively. Whereas shorter-period waves do not see the assumed thicker transition zone as expected, longer-period waves can see it better as its thickness increases. In the frequency range from 0.0 to 0.2 Hz, however, variations in $R(\omega)$ and $T(\omega)$ are less than 25 per cent, and 0.5 sec for each of the above models. The change in phase spectrum, $\omega T(\omega)$ in this frequency range is about 0.11 (6°), 0.28 (16°), and 0.56 (32°), respectively. We may neglect these amounts of amplitude and phase variations. Although these variations become more noticeable with increased i_c, and accordingly larger epicentral distance, the signal amplitude of the *PcP* phase is negligibly small over the distance range of over about 55°, as apparent from comparisons of the *P* and *PcP* phases in Kanamori (1967), Buchbinder (1968), and Kurita (1972b). Thus, we may expect that expression (13) can be a sufficiently accurate expression with appropriate estimates for a and t_{PcP-P}. These factors should be experimentally estimated from observed records and/or spectra with the aid of theoretical values for g and C, and predicted travel-time difference. Incorporating the *pP* and *PcP* phases into the record section of the *P* phase, Hasegawa (1971) calculated theoretical amplitude ratios and compared them with observed ones, but could not succeed in getting a good fit. He assumed the same spectral structure with equal amplitude for *P*, *PcP*, and *pP* phases.

So far we have been concerned with records of deep-focus earthquakes, which in most cases can be expected only from limited directions. Elucidation of the detailed structure from spectra of shallow earthquakes is almost impossible, because the effect of $M(\omega)$ cannot be easily discriminated from that of $L(\omega)$, and $M(\omega)$ may couple with $S(\omega)$. However, by analyzing records of shallow earthquakes with various focal depths, we can study azimuthal variations in crustal structure around the station, as done by Kurita (1972a).

S phase. Figure 8 shows travel-time differences between the direct *S* phase and most of the preceding and later phases arriving within 1 min before and 4 min after the direct *S* phase for focal depths of 300 and 600 km. Time differences are calculated from tables of Shimshoni (1966) for *SP*, *PS*, and *SS*, Jeffreys and Shimshoni (1964) for *pS* and *sS*, and Jeffreys and Bullen (1940) for *SPP*, *PPS* (or *PSP*), *ScS*, *SKS*, SKS_2, and *SKKS*. Calculation of time differences for *PcS*, *ScP*, *pPcP*, *sPcP*, *pPcS*, *sScP*, *pScS*, *sScS*, *pSKS*, and *G* are based on travel-time curves of Gutenberg and Richter (1936). *pPS* (or *pSP*) is possible for the focal depth of 300 km but is not shown. The situation surrounding the direct *S* phase is rather complicated. The most troublesome are *SP* and *SPP* which closely follow it, and core phases also usually precede and/or follow it. Together with the longer time length required for *S* waves, the utilization of *S*-wave spectra is seemingly not hopeful. However, it depends on whether these phases strongly affect the *S* phase or not. It seems through the actual analysis made by Kurita (1972b) that *S* waves are useful at least for the verification of models inferred from *P* waves.

Effect of Noise on the Transfer Ratio

Apart from the so-called signal-generated noise, we can limit our discussion to the background noise.

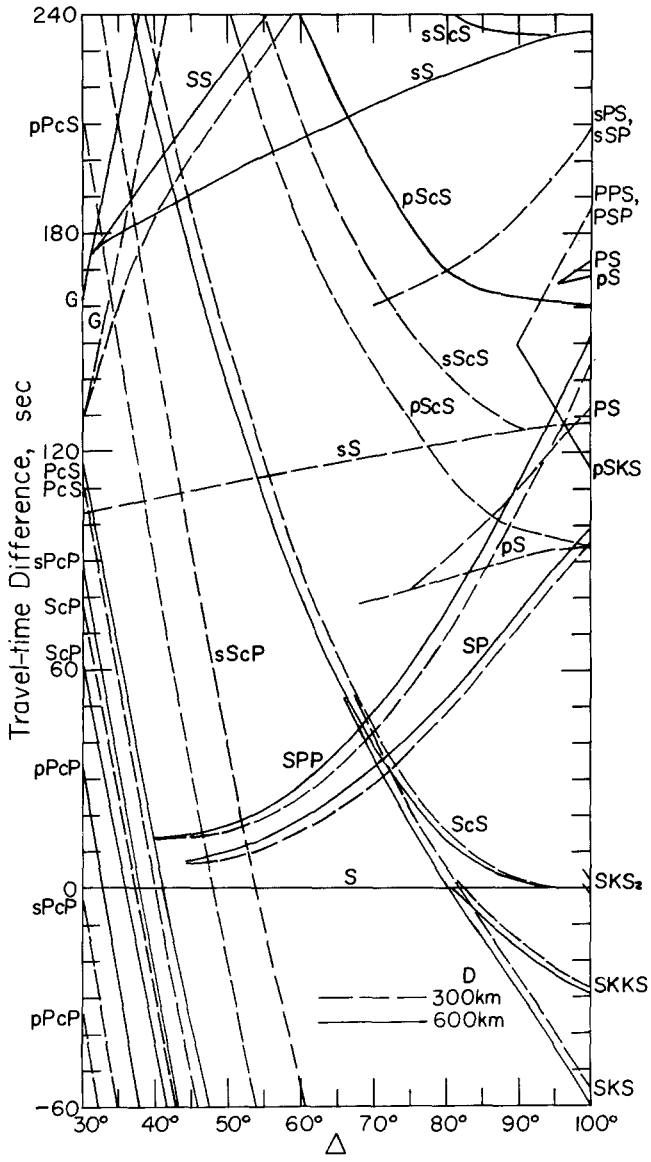

FIG. 8. Travel-time differences between the teleseismic direct *S* phase and most of the preceding and later phases for focal depths of 300 and 600 km.

As observed in the actual analysis of Kurita (1972b), the existence of noise in the signal usually sharpens spectral peaks, postulating abrupt velocity contrasts in the structure. Since the *P* and *S* phases are seldom free from the contamination from the background noise, we could bring the effect of noise into formula (1). However, difference in noise spectra among records makes it impossible to superpose observational transfer ratios. Therefore, we prefer analyzing records with and without the noise and estimating its effect, and/or later incorporating the noise into synthetic seismograms in the procedure shown in the next section.

Effect of the Deviation of the Direction of Wave Approach on the Transfer Ratio

The pure longitudinal trace, $f_L(t, \phi)$, and the pure transverse trace, $f_T(t, \phi)$, are obtained from the NS record, $f_N(t)$, and the EW record, $f_E(t)$, by transformations

$$f_L(t, \phi) = f_N(t) \cos \phi + f_E(t) \sin \phi \tag{14}$$

$$f_T(t, \phi) = f_N(t) \sin \phi - f_E(t) \cos \phi \tag{15}$$

where $f_L(t, \phi)$ is taken positively away and $f_T(t, \phi)$ to the right of the path from the epicenter, respectively, and ϕ is the direction of wave approach. The transverse amplitude of P waves for the relevant geometrical azimuth estimated from expression (15) should be zero if the underlying structure consists of horizontal parallel layers. However, even for long-period records, a considerable transverse energy is sometimes observed (Kurita, 1972b). This may be a combined effect caused by deviation of the direction of wave approach from the geometrical azimuth together with scattering in the layers and noise. A simple approach for estimating the possible deviation is to calculate the ratio of energy contained in the transverse motion to the total energy in the relevant wave. According to Parseval's theorem, the energy which is proportional to the integral of the square of the signal amplitude, $f(t, \phi)$, is equal to that of the amplitude spectrum of the signal, $|F(\omega, \phi)|$,

$$\int_{\infty}^{-\infty} f(t, \phi)^2 \, dt = \frac{1}{2\pi} \int_{-\infty}^{\infty} |F(\omega, \phi)|^2 \, d\omega.$$

Inasmuch as an elimination of the instrumental effect is easier in the frequency domain than in the time domain, we prefer estimating this integral in the frequency domain. By varying the direction of wave approach around the geometrical azimuth, we can estimate the ratio of the transverse energy to the total energy, $E_r(\phi)$

$$E_r(\phi) = \int_{\omega_1}^{\omega_2} |F_T(\omega, \phi)|^2 \, d\omega \Big/ \int_{\omega_1}^{\omega_2} \{ |F_L(\omega, \phi)|^2 + |F_T(\omega, \phi)|^2 \} \, d\omega \tag{16}$$

where $|F_L(\omega, \phi)|$ and $|F_T(\omega, \phi)|$ are the longitudinal and transverse amplitude spectra, respectively, and ω_1 and ω_2 are the initial and final circular frequencies between which the integral is evaluated. ϕ corresponding to the minimum value of $E_r(\phi)$ may be regarded as true direction of wave approach, and the deviation of this direction from the geometrical azimuth may give a measure for the true deviation. By comparing the observational transfer ratios for this direction and the geometrical azimuth, we can evaluate the effect of this deviation, including the effect resulting from the possible mislocation of the epicenter.

Although in the above we have not been concerned with the anelastic property of the media in the layered structure, it will be taken into account in the actual analysis when it is necessary (Kurita, 1973b).

Procedure for the Study of the Crustal and Upper Mantle Structure

Ben-Menahem, Smith, and Teng (1965) proposed a routine procedure for elucidating source parameters of deep-focus earthquakes from the spectral analysis of long-period body waves. Their procedure aims to elucidate the source process from the source spectrum by the removal of propagation effects, whereas we need the source spectrum to clarify the detailed layered structure. Fuchs (1970) proposed a procedure to investigate the layered structure by an iterative study of travel-time, dispersion, crustal response, and synthetic seismogram. With the aid of the actual analyses of Kurita (1972a, b, c, d), we have constructed the procedure shown in Figure 9 which may be regarded as an

improved version of his. In our procedure, the transfer ratio method is in the heart because it is the most effective among the methods. The possible flow of the procedure is indicated by arrows. Methods in larger squares are connected by shorter arrows to the resultant models in smaller squares, whereas a dotted arrow points to a by-product. "Surface wave" includes all or some of phase and/or group-velocity dispersion studies of Rayleigh and/or Love waves. "Surface wave (1)" or "(2)" may be associated with wave periods shorter or longer than about 30 sec, respectively. "Travel-time" is concerned with all or some kind of travel-time studies, including a study on amplitude variation with distance. "Travel-time (1)" may be mainly associated with refraction surveys, whereas "travel-time (2)" may be mainly associated with a derivative of travel-time and/or travel-time residual studies. Each method should be processed in accordance with the quality of data concerned, sometimes discarding data of low quality.

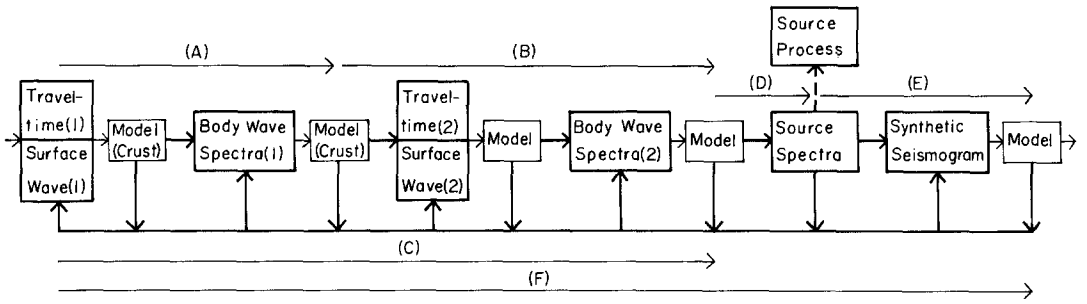

FIG. 9. Schematic representation of an iterative procedure proposed for the detailed study of the crustal and upper-mantle structure. The possible flow of the procedure is indicated by arrows. Large squares enclose methods, and small squares include the resultant models. Letters correspond to steps in the text.

The following six steps represent the minimum path required to construct the fine layered model.

(A) Based mainly on refraction surveys made near the station of which data are to be analyzed, we assume a preliminary velocity-density model for the crust, process the first step of the two-step procedure, and construct the crustal model.

(B) Based mainly on surface-wave dispersion and/or travel-time studies so far made for the area concerned, we assume a velocity-density model of the upper mantle below the crustal model obtained in step A, process the second step, and construct the layered model for the upper mantle.

(C) Travel-time and surface-wave dispersion studies are made, in which data may be adopted from studies so far made. The model is adjusted to be consistent with all data up to this step.

(D) The source spectrum, or the spectrum of the wave incident at the base of the resultant model, is derived by compensating propagation effects.

(E) A synthetic seismogram based on the resultant model and source spectrum is compared with the seismogram observed at the station. If the matching of both seismograms is unsatisfactory, the parameters of the model are adjusted. In synthesizing seismograms, effects from noise and preceding and/or later phases, if necessary, may be incorporated. Inasmuch as the direct S phase is usually disturbed by surrounding phases, S-wave study in the time domain may sometimes be preferred to that in the frequency domain.

(F) The resultant model is adjusted to be consistent with all data.

Because each method lacks uniqueness in determining the layer parameters, in each step, we may prefer to set up the possible range for the values of the parameters of the models, rather than to obtain one or two models with definite values of the parameters and pass these values to the next step.

Acknowledgments

The author is grateful to Charles B. Archambeau for valuable discussions throughout this study. He is also indebted to Don L. Anderson, Bernard Minster, and James H. Whitcomb for their critical reviews of the manuscript. Unpublished core-mantle boundary model was provided by Don L. Anderson and Thomas H. Jordan. This research was supported by the Advanced Research Projects Agency and monitored by the Air Force Office of Scientific Research under Contracts Nos. F44620-69-C-0067 and F44620-72-C-0078.

References

Anderson, D. L. and T. H. Jordan, (1972). The structure, composition and evolution of the earth's interior, *Eos, Trans. Am. Geophys. Union* **53,** 451.

Archambeau, C. B. (1968). General theory of elastodynamic source fields, *Rev. Geophys.* **6,** 241–288.

Archambeau, C. B., E. A. Flinn, and D. G. Lambert (1969). Fine structure of the upper mantle, *J. Geophys. Res.* **74,** 5825–5865.

Bakun, W. H. (1971). Crustal model parameters from *P*-wave spectra. *Bull. Seism. Soc. Am.* **61,** 913–935.

Ben-Menahem, A., S. W. Smith, and T. L. Teng (1965). A procedure for source studies from spectrums of long-period seismic body waves, *Bull. Seism. Soc. Am.* **55,** 203–235.

Berzon, I. S. (1965). The determination of a model of a thinly layered medium by the simultaneous use of amplitude- and phase-spectrum characteristics of the layer, *Bull. Acad. Sci. SSSR, Ser. Geophys. (English Transl.)* 363–367.

Bolt, B. A. (1972). Structure of the earth's core from seismological evidence, *Eos, Trans. Am. Geophys. Union* **53,** 599.

Bonjer, K. P., K. Fuchs, and J. Wohlenberg (1970). Crustal structure of the East African Rise System from spectral response ratios of long-period body waves, *Z. Geophys.* **36,** 287–297.

Buchbinder, G. G. R. (1968). Amplitude spectra of *PcP* and *P* phases, *Bull. Seism. Soc. Am.* **58,** 1797–1819.

Ellis, R. M. and Basham, P. W. (1968). Crustal characteristics from short-period *P* waves, *Bull. Seism. Soc. Am.* **58,** 1681–1700.

Espinosa, A. F., G. H. Sutton, and H. J. Miller (1965). A transient technique for seismograph calibration in *Manual and Standard Set of Theoretical Transient Responses*, Geophysics Laboratory, The Univeristy of Michigan.

Ewing, W. M., W. S. Jardetzky, and F. Press (1957). *Elastic Waves in Layered Media*, McGraw-Hill, New York.

Fernandez, L. M. and J. Careaga (1968). The thickness of the crust in central United States and La Paz, Bolivia, from the spectrum of longitudinal seismic waves, *Bull. Seism. Soc. Am.* **58,** 711–741.

Fuchs, K. (1970). On the determination of velocity depth distributions of elastic waves from the dynamic characteristics of the reflected wave field, *Z. Geophys.* **36,** 531–548.

Glover, P. and S. S. Alexander (1969). Lateral variations in crustal structure beneath the Montana LASA, *J. Geophys. Res.* **74,** 505–531.

Green, R. W. E. and A. L. Hales (1968). The travel times of *P* waves to 30° in the central United States and upper mantle structure, *Bull. Seism. Soc. Am.* **58,** 267–289.

Gutenberg, B. and C. B. Richter, (1936). Travel-times, Seismological Laboratory, California Institute of Technology.

Hales, A. L., C. E. Helsley, and J. B. Nation (1970). *P* travel times for an oceanic path, *J. Geophys. Res* **75,** 7362–7381.

Hasegawa, H. S. (1970). Short-period *P*-coda characteristics in the eastern Canadian Shield, *Bull. Seism. Soc. Am.* **60,** 839–858.

Hasegawa, H. S. (1971). Crustal transfer ratios of short- and long-period body waves recorded at Yellowknife, *Bull. Seism. Soc. Am.* **61,** 1303–1320.

Helmberger, D. and R. A. Wiggins (1971). Upper mantle structure of midwestern United States, *J. Geophys. Res.* **76,** 3229–3245.

Herrin, E. *et al.* (1968). 1968 seismological tables for *P* phases, *Bull. Seism. Soc. Am.* **58,** 1193–1241.

Hill, D. P. (1971). Crustal and upper mantle structure of the Columbia Plateau from long-range seismic refraction measurements (in press).

Ishii, H. and R. M. Ellis (1970). Multiple reflection of plane P and SV waves by a dipping layer, *Geophys. J.* **20,** 11–30.

Jeffreys, H. and K. E. Bullen (1940), *Seismological Tables*, Brit. Assoc. Advancement of Sci., Gray-Milne Trust.

Jeffreys, H. and M. Shimshoni (1964). The times of pP, sS, sP and pS, *Geophys. J.* **8,** 324–337.

Johnson, L. R. (1967). Array measurements of P velocities in the upper mantle, *J. Geophys. Res.* **72,** 6309–6325.

Johnson, L. R. (1969). Array measurements of *P* velocities in the lower mantle, *Bull. Seism. Soc. Am.* **59,** 973–1008.

Jordan, T. H. and D. L. Anderson (1972). Differential travel times for gross earth studies, *Eos, Trans. Am. Geophys. Union* **53,** 453.

Julian, B. R. (1970). Regional variations in the upper mantle structure beneath North America, *Ph.D. Thesis*, Californria Institute of Technology.

Julian, B. R. and D. L. Anderson (1968). Travel times, apparent velocities, and amplitudes of body waves, *Bull. Seism. Soc. Am.* **58,** 339–366.

Kanamori, H. (1967). Spectrum of P and PcP in relation to the mantle-core boundary and attenuation in the mantle. *J. Geophys. Res.* **72,** 559–571.

Kane, J. (1965). Travel time and phase shift, *J. Geophys. Res.* **70,** 1893–1895.

Kurita, T. (1968). Attenuation of short-period P-waves and Q in the mantle, *J. Phys. Earth* **15,** 61–78.

Kurita, T. (1969a). Crustal and upper mantle structure in Japan from amplitude and phase spectra of long-period P-waves, Part 1. Central mountain area, *J. Phys. Earth* **17,** 13–41.

Kurita, T. (1969b). Crustal and upper mantle structure in Japan from amplitude and phase spectra of long-period P-waves, Part 2. Kanto plain, *Special Contributions, Geophys. Inst., Kyoto Univ.* **9,** 137–166.

Kurita, T. (1969c). Spectral analysis of seismic waves, Part 1. Data windows for the analysis of transient waves, *Special Contributions, Geophys. Inst., Kyoto Univ.* **9,** 97–122.

Kurita, T. (1970). Crustal and upper mantle structure in Japan from amplitude and phase spectra of long-period P-waves, Part 3. Chugoku region, *J. Phys. Earth* **18,** 53–78.

Kurita, T. (1971). Inferences of a layered structure from S wave spectra, Part 2. Study of the structure in selected regions of Japan, *J. Phys. Earth* **19,** 111–142.

Kurita, T. (1972a). Regional variations in the structure of the crust in the central United States from P wave spectra, *J. Phys. Earth* **20,** (in press).

Kurita, T. (1972b). Upper mantle structure in the central United States from P and S wave spectra, *J. Phys. Earth* **20,** (in press).

Kurita, T. (1972c). Upper mantle structure in the western United States, *Eos, Trans. Am. Geophys. Union* **53,** 1045.

Kurita, T. (1973a). Source time functions of some deep earthquakes which occurred in South America, (in preparation).

Kurita, T. (1973b). Crustal and upper mantle structure in the central United States from surface-wave dispersion, travel-times, and synthetic seismograms, (in preparation).

Kurita, T. and T. Mikumo (1971). Inferences of a layered structure from *S* wave spectra, Part 1. Theoretical considerations of *S* wave spectrum method, *J. Phys. Earth* **19,** 93–110.

Leblanc, G. S. J. (1967). Truncated crustal transfer functions and fine crustal determination, *Bull. Seism. Soc. Am.* **57,** 719–733.

Lewis, B. T. R. and R. P. Meyer (1968). A seismic investigation of the upper mantle to the west of Lake Superior, *Bull. Seism. Soc. Am.* **58,** 565–596.

Mereu, R. F. and J. A. Hunter (1969). Crustal and upper mantle structure under the Canadian Shield from project Early Rise data, *Bull. Seism. Soc. Am.* **59,** 147–165.

Mikumo, T. and T. Kurita (1971). Inferences of a layered structure from *S* wave spectra, Part 3. *SH* and *SV* waves and some related problems, *J. Phys. Earth* **19,** 243–257.

Phinney, R. A. (1964). Structure of the earth's crust from spectral behavior of long-period body waves *J. Geophys. Res.* **69,** 2997–3017.

Phinney, R. A. (1972). Seismological evidence on the core-mantle boundary, *Eos, Trans. Am. Geophys. Union* **53,** 600.

Ritsema, A. R. (1958). $(i-\Delta)$-curves for bodily seismic waves of any focal depth, *Meteorol. and Geophys. Inst. Djakarta, Verhandel.* **54,** 1–10.

Rogers, Jr., A. M. and C. Kisslinger (1972). The effect of a dipping layer on *P*-wave transmission, *Bull. Seism. Soc. Am.* **62,** 301–324.

Roller, J. C. and W. H. Jackson (1966). Seismic-wave propagation in the upper mantle: Lake Superior, Wisconsin to Denver, Colorado, *Am. Geophys. Union, Geophys. Mon., Ser. 10,* 270–275.

Sato, R. (1969). Amplitudes of *PcP* and *PcS* obtained from ray and wave theory solutions and amplitudes near shadow boundary, *J. Phys. Earth* **17,** 1–12.

Shimshoni, M. (1966). The times of *PP*, *SS*, *SP* and *PS*, *Geophys. J.* **11,** 477–483.

Shimshoni, M. and A. Ben-Menahem (1970). Computation of divergence coefficient for seismic phases, *Geophys. J.* **21,** 285–294.

Stauder, W. and O. W. Nuttli (1970). Seismic studies: south central Illinois earthquake of November 9, 1968, *Bull. Seism. Soc. Am.* **60,** 973–981.

Teng, T. L. (1967). Reflection and transmission from a plane layered core-mantle boundary, *Bull. Seism. Soc. Am.* **57,** 477–499.

Teng, T. L. and A. Ben-Menahem (1965). Mechanism of deep earthquakes from spectrums of isolated body-wave signals, 1. The Banda Sea earthquake of March 21, 1964, *J. Geophys. Res.* **70,** 5157–5170.

Whitcomb, J. H. and D. L. Anderson (1970). Reflection of *P'P'* seismic waves from discontinuities in the mantle, *J. Geophys. Res.*, **75,** 5713–5728.

Wu, F. T. and W. J. Hannon (1966). *PP* and crustal structure, *Bull. Seism. Soc. Am.* **56,** 733–747.

Seismological Laboratory
California Institute of Technology
Pasadena, California 91109
Contribution 2180 of the Division of
Geological and Planetary Sciences

Manuscript received June 16, 1972